HHS Public Access

Author manuscript

Chemosphere. Author manuscript; available in PMC 2022 April 01.

Published in final edited form as:

Chemosphere. 2021 April ; 269: 128773. doi:10.1016/j.chemosphere.2020.128773.

Sub-chronic microcystin-LR renal toxicity in rats fed a high fat/high cholesterol diet

Tarana Arman[1], **Katherine D. Lynch**[1], **Michael Goedken**[2], **John D. Clarke**[1,*]

[1]Department of Pharmaceutical Sciences, Washington State University, Spokane, WA 99202, USA

[2]Department of Pharmacology and Toxicology, Rutgers University, Piscataway, NJ 08901, USA

Abstract

Microcystin-LR (MCLR) is a liver and kidney toxin produced by cyanobacteria. Recently, it was demonstrated that MCLR exposure drives the progression of high fat/high cholesterol (HFHC) induced nonalcoholic fatty liver disease (NAFLD) to a more severe state. NAFLD is also a risk factor for chronic kidney disease (CKD), and the current study investigated MCLR renal toxicity in the context of an HFHC diet. Sprague Dawley rats were fed either a control diet or an HFHC diet for 10 weeks. After 6 weeks of diet, animals were administered either vehicle, 10 μg/kg, or 30 μg/kg MCLR *via* intraperitoneal injection every other day for 4 weeks. HFHC diet alone increased the renal glomerular change histopathology score, and 30 μg/kg MCLR exposure increased this score in both the control group and the HFHC group. In contrast, 30 μg/kg MCLR caused greater proteinuria and cast formation and decreased protein phosphatase 1 and 2A protein expression in the HFHC group. Urinary excretion of KIM-1 increased, but albumin and tamm-horsfall protein did not change after MCLR exposure. The general concordance between KIM-1, polyuria, proteinuria, and renal casts after MCLR exposure suggests that proximal tubule cell damage contributed to these connected pathologies. The control group adapted to repeated MCLR exposure by increasing the urinary elimination of MCLR and its metabolites, whereas this adaptation was blunted in the HFHC group. These data suggest an HFHC diet may increase the severity of certain MCLR-elicited renal toxicities.

*Correspondence: Dr. John Clarke, Assistant Professor, Pharmaceutical Sciences, j.clarke@wsu.edu; Tel.: +1-509-358-792, 412 E Spokane Falls Blvd, PBS 343, Spokane, WA 99202.

CRediT authorship contribution statement

Tarana Arman: Conceptualization, Investigation, Methodology and Formal analysis, Writing- original draft, Writing- review and editing, Visualization; **Katherine D. Lynch**: Investigation, Methodology and Formal analysis, Writing- review and editing; **Michael Goedken**: Methodology and Formal analysis, Writing- review and editing, Visualization; **John D. Clarke**: Conceptualization, Investigation, Writing-original draft, Writing- review and editing, Supervision, Project administration, Funding acquisition

Declaration of interests

The authors declare that they have no known competing financial interests or personal relationships that could have appeared to influence the work reported in this paper.

Keywords

chronic kidney disease (CKD); KIM-1; microcystin; nonalcoholic fatty liver disease (NAFLD); proteinuria

1. Introduction:

Microcystin-leucine arginine (MCLR) is a cyclic heptapeptide produced by prokaryotic photosynthetic bacteria that is known to cause liver and kidney toxicities in human populations (Paerl and Paul, 2012; Svirčev et al., 2017). MCLR is primarily a hepatotoxin because it is substrate for the liver specific organic anion transporting polypeptide-1B (OATP1B) transporters (Oatp1b2 in rodents and OATP1B1/OATP1B3 in humans) (Clarke et al., 2019; Fischer et al., 2010, 2005). MCLR is also a renal toxin and its primary metabolites, MCLR-glutathione (MCLR-GSH) and MCLR-cysteine (MCLR-Cys), accumulate in rodent kidney after MCLR exposure (Ito et al., 2002). The specific molecular, cellular, and physiological processes perturbed by MCLR are influenced by MCLR exposure level and duration, with higher acute or sublethal exposures causing necrosis and lower chronic exposures causing tumor promotion (Svirčev et al., 2017).The common molecular mechanisms of MCLR liver and kidney toxicity include inhibition of serine-threonine protein phosphatase-1 (PP1) and PP2A, production of reactive oxygen species, disruption of cytoskeleton, and inflammation (Abdel-Daim et al., 2019; AlKahtane et al., 2020; Campos and Vasconcelos, 2010; Liang et al., 2011; Liu and Sun, 2015). MCLR disrupts protein phosphatase activity by covalently binding to the active site of the enzyme, requiring production of new protein to restore PP1 and PP2A activity (Xing et al., 2006). Data from rodent studies indicate that MCLR renal toxicity presents as glomerular damage, altered creatinine clearance, and proteinuria (Milutinović et al., 2003; Nobre et al., 2001; Yi et al., 2019). A recent cross-sectional study in China reported that higher estimated MCLR exposure was associated with abnormal blood urea nitrogen, serum creatinine, and estimated glomerular filtration rate (Lin et al., 2016). Most MCLR rodent studies, including the studies that determined the current MCLR Tolerable Daily Intake (TDI) value, were performed in healthy animals (Fawell et al., 1999), but there is increasing interest in identifying at-risk populations who may be more susceptible to MCLR-induced liver and kidney toxicities, such as individuals with underlying liver and/or kidney diseases.

Chronic kidney disease (CKD) affects approximately 30 million adults in the United States and has an estimated global prevalence of 13.4% (Coresh, 2017; Hill et al., 2016; Levey et al., 2007; Mills et al., 2015; Targher et al., 2008; Targher and Byrne, 2017). CKD is characterized by progressive loss of kidney function, specifically decreased glomerular filtration and/or increased proteinuria (Webster et al., 2017). It is generally associated with obesity, diabetes, hypertension (Soderland et al., 2010), and shares cardio-metabolic risk factors with nonalcoholic fatty liver disease (NAFLD) (Ibrahim et al., 2016; Laurentius et al., 2019; Targher et al., 2011). Multiple cohort studies indicate NAFLD patients have higher CKD incidence compared to non-NAFLD patients (Hill et al., 2016; Kramer and Luke, 2007; Musso et al., 2014; Sinn et al., 2017). Occupational and environmental exposure to toxins also contribute to the burden of both CKD and NAFLD (Arman et al., 2019; Craig et

al., 2015; Kataria et al., 2015; Soderland et al., 2010; Wahlang et al., 2014, 2013). We previously demonstrated that MCLR exposure drives high-fat/high-cholesterol (HFHC) diet induced NAFLD towards more severe liver pathology (Arman et al., 2019). Given the association between NAFLD and CKD, we hypothesized that MCLR would also exacerbate renal toxicity. Data presented here indicate that MCLR exposure exacerbates specific aspects of HFHC-associated kidney disease.

2. Materials and Methods:

2.1. Animals and treatments:

Eight-week-old male Sprague-Dawley rats (n=36) were purchased from Envigo (Huntingdon, Cambridgeshire, UK). All animals were maintained in 12 h light and dark cycles for the duration of the study. Animals were divided into two groups and fed either a control diet (Dyets Inc., Bethlehem, PA, USA, Catalog# 518754) or an HFHC diet (Research Diets, New Brunswick, NJ, USA, Catalog# D06061401) for 6 weeks. Animals were then divided into three treatment groups (n=6 per group) and dosed with intraperitoneal injections of either vehicle (0.9% saline, 0.09% ethanol; 5 mL/kg) or MLCR (10 μg/kg or 30 μg/kg; 5 mL/kg; Cayman Chemicals [Ann Arbor, MI, USA]) every 48 h for 4 weeks (10 weeks total on diets). Blood was collected from the tail vein into heparinized tubes prior to the first MCLR dose (day 0), 24 h after the seventh dose (day 14), and 24 h after the last dose (day 29). Blood was centrifuged at 10,000 × g for 5 min at 4°C and plasma was removed and stored at −80°C until further analysis. Animals were housed in metabolic cages from 24 h before until 24 h after, the first and last MCLR doses (48 h housing duration each time). Total urine was collected from the rats during the following time intervals: 0 to 6 h, 6 to 12 h and 12 to 24 h after MCLR intraperitoneal injection and stored at −80 °C. 24 h after the final MCLR injection, rats were euthanized by carbon-dioxide asphyxiation, tissues were harvested and were formalin fixed and snap frozen. Handling, care and maintenance of the animals was done in the Association for the Assessment of Laboratory Animal Care International accredited program of the Laboratory Animal Resources facility of Washington State University, Spokane. All aspects of the animal research were approved by the Institutional Animal Care and Use Committee at Washington State University (approval code 04937, 14 December 2016).

2.2. Proteinuria quantification

Urine protein concentration was measured using the Pierce BCA Protein Quantification Assay kit (Thermo Fisher Scientific, Waltham, MA, USA) according to the manufacturer's protocol (Catalog# 23225). Proteinuria was calculated from the protein concentration in urine multiplied by the total urine volume per unit time (h).

2.3. Urinary kidney injury molecule-1 (KIM-1) quantification

Urinary KIM-1 was measured using the Rat KIM-1 PicoKine™ ELISA Kit (Boster Biological Technology, Pleasanton, CA, USA) as per the manufacturer's protocol (Catalog# EK0882). The urinary KIM-1 was calculated from the KIM-1 concentration in urine multiplied by the total urine volume per unit time (h).

2.4. Creatinine clearance

Plasma and urine creatinine concentrations were assessed with colorimetric kits according to manufacturer's protocols (Catalog# 700460 and Catalog# 500701, respectively; Cayman Chemicals, Ann Arbor, MI, USA). Creatinine clearance was calculated using the following formula:

$$\text{Creatinine clearance (ml/min)} = (\text{Urine creatinine} \times \text{Urine volume}) / (\text{Serum creatinine} \times 1440)$$

2.5 Histopathological Analysis

Formalin fixed kidney tissues were processed, paraffin embedded, sectioned at 4 μm, stained with hematoxylin and eosin (H&E) or immunohistochemistry was performed for Bcl-2 (Novus Biologicals, Littleton, CO, USA, Catalog# NB100–56101), Bax (Novus Biologicals, Catalog# NBP1–28566), and Caspase-8 (Novus Biologicals, Catalog# NB100–56116). The H&E stained slides were examined by a board-certified veterinary pathologist. Incidence and severity score criteria were as follows: 0, no noteworthy lesions (0%); 1, minimal (<10%); 2, mild (10%–25%); 3, moderate (25%–40%); 4, marked (40%–50%); 5, severe (>50%).

2.6. Protein Preparations

Approximately 50 mg of kidney tissue was homogenized with NP40 lysis buffer with protease inhibitors (Catalog# PI88665, Thermo Fisher Scientific, Waltham, MA, USA). Homogenized samples were agitated at 4°C for 2 h and then centrifuged at 10,000x g at 4°C for 1 h. Supernatants were collected and Protein concentrations were determined from supernatant using the Pierce BCA Protein Quantification Assay kit (Thermo Fisher Scientific, Waltham, MA, USA).

2.7. Immunoblot Protein Analysis

Twenty micrograms of total protein from kidney tissue lysates were prepared in Laemmli buffer with 2.5% β-(BME) and heated at 37°C for 30 min. Samples were loaded into either 7.5% gels prepared with TGX FastCast Acrylamide Solutions (Bio-Rad, Hercules, CA, USA) or 12% SDS-PAGE gels to probe for PP2A and MCLR or PP1, respectively. For tamm-horsfall protein (THP), 50 μg of total protein from kidney tissue lysates were prepared in Laemmli buffer with 2.5% BME without heat and samples were loaded into 7.5% SDS-PAGE gels. Protein was transferred from gels to polyvinylidene fluoride (PVDF) membranes with a Bio-Rad (Hercules, CA) Trans-Blot Turbo system at 25V/1.0 A for 30 min. Following transfer, the blots were blocked with 5% non-fat dry milk in Tris-base buffered saline-Tween 20 (TBS-T) and incubated with following antibody conditions: PP2A (1: 2,000 dilution; Millipore, Burlington, MA, USA) (Catalog# 05–421; 1:10,000 mouse secondary), MCLR (1:2,000 dilution; Enzo, Farmingdale, NY, USA) (Catalog# 89154–022; 1:10,000 mouse secondary), PP1 (1:1,000 dilution; Santa Cruz Biotechnology, Santa Cruz, CA, USA) (Catalog# sc-7482; 1:10,000 mouse secondary), THP (1:5,000 dilution; Santa Cruz Biotechnology, Santa Cruz, CA, USA) (Catalog# sc-271022; 1:10,000 mouse secondary).

THP and albumin proteins were probed in urine samples. Urine samples containing 0.51 μg (THP immunoblotting) and 0.08 μg (Albumin immunoblotting) of creatinine were prepared in Laemmli buffer with 2.5% BME without heat. The samples were loaded into 7.5% SDS-PAGE gels. Transfer to PVDF membrane and blocking were done as described above. Antibody conditions used for incubation are as follows: THP (1:1,000 dilution; Santa Cruz Biotechnology, Santa Cruz, CA, USA) (Catalog# sc-271022; 1:10,000 mouse secondary) and albumin (1:2,000 dilution; Santa Cruz Biotechnology, Santa Cruz, CA, USA) (Catalog# sc-271605; 1:10,000 mouse secondary).

Chemiluminescence was developed with SuperSignal West Pico PLUS (Thermo Fisher Scientific, Waltham, MA, USA) and images were captured using a Bio-Rad ChemiDoc imager. Densitometry was performed using Image Lab (Bio-Rad, Standard Edition, Version 6.0.0 build 25). Proteins of interest were normalized to total protein stained with Amido Black. Total protein normalization is a commonly accepted technique for protein densitometry analysis instead of a single-protein loading control (Aldridge et al., 2008; Arman et al., 2019).

2.8. mRNA Expression and qPCR quantification

Total RNA was extracted from rat kidney using TRIzol reagent (Thermo Fisher Scientific, Waltham, MA, USA) according to manufacturer's protocol (Catalog# 15596018). RNA concentrations were determined using a nano-drop, and RNA integrity was confirmed by agarose gel electrophoresis. iScript cDNA synthesis kit (Bio-Rad, Hercules, CA, USA) (Catalog# 1708841) was used for cDNA synthesis from total RNA, and PerfeCTa SYBR Green SuperMix, ROX (Quantabio, Beverly, MA, USA) (Catalog# 101414–160) was used for real time quantitative PCR analysis as per manufacturer's protocol. Primers were purchased from Sigma (St. Louis, MO, USA) for the following genes: Solute Carrier Family 47 Member 1 (*Slc47a1*) or MATE1 (NM_001014118.2) forward CTGTCTGGCTTTCAAGAGGAG, reverse CAGAGGAGCAGGATGAGTGTC; Solute Carrier Family 47 Member 2 (*Slc47a2*) or MATE2 (NM_001191920.1) forward CAAGTGATGCCCATTTTTGCTC, reverse AGAGGGCTTGGAAGAAGACAC; Solute Carrier Family 12 member 1 (*Slc12a1*) or NKCC2 (NM_001270618.1) forward GTCATCATCATTGGCCTGAGCG, reverse AAGGTCTACCACAGTCTCCGC; LDL Receptor related Protein 2 (*Lrp2*) or Megalin (NM_030827.1) forward ACTGCACTACCCTGTGTTCG, reverse AGGACACGCCCATTCTCTTG; Cubilin (*Cubn*) (NM_053332.2) forward ACAAGAAGGAAGGCGGATCG, reverse TTTCCACCGGAGACACTTGG; Solute carrier family 22 member 2 (*Slc22a2*) or OCT2 forward TCTTGATGTACAATTGGTTCACG, reverse AACCACAGCAAATACGACCAG (More et al., 2010); Vimentin (*Vim*) (NM_031140.1) forward GGCACGTCTTGACCTTGAAC, reverse GGCTTGGAAACGTCCACATC; Tumor necrosis factor (*Tnfα*) (NM_012675.3) forward ACTACGATGCTCAGAAACAC, reverse AATAGAGGGGGTTCCGTAAG; Interleukin 10 (*IL10*) (NM_012854.2) forward TCCCCTGTGAGAATAAAAGC, reverse ATGTCAAACTCATTCATGGC; Interleukin 1-beta (*IL1β*) (NM_031512.2) forward TGTGGATCCCAAACAATACC, reverse ATAGTGCAGCCATCTTTAGG; and Glyceraldehyde-3-phosphate dehydrogenase (*Gapdh*) (NM_017008) forward CTTGTGCAGTGCCAGCCTC, reverse

TCCCGTTGATGACCAGCTTC; and Beta-2 microglobulin (*β2m*) (NM_012512.2) forward TGTGGCTGGAGGTTTAGTCC, reverse AACAGAAGGGCAGAAGACGC and mitogen-activated protein kinase (*Mapk*) (NM_053842.2) forward CTACGGCATGGTTTGTTCTG, reverse ATCTGCTCAATGGTTGGTGC. The expression for the genes of interest were normalized to the average expression of three housekeeping genes (*Gapdh, β2M* and *Mapk*).

2.9. MCLR quantification

The parent MCLR and the MCLR metabolites (MCLR-GSH and MCLR-Cys) were quantified with urine collected after the first and the last MCLR dose using a previously published protocol (Montonye et al., 2019).

2.10. Statistical analysis

All results are represented as mean ± SD. All data, except the semi quantitative histopathological data, were analyzed by two-way ANOVA statistical analysis with diet and dose constituting the main two factors. Dunnett and Sidak's multiple comparison post-tests were performed to determine statistical differences between different treatment groups. All analyses were carried out using GraphPad Prism software. (GraphPad Software, Inc., La Jolla, CA, USA).

3. Results and Discussion:

3.1. Kidney weight and pathology after MCLR exposure

Changes in organ weight and organ-to-body weight ratio are sensitive biomarkers of organ toxicity, (Michael et al., 2007) and altered absolute kidney weight correlates with greater severity of histopathology endpoints (Craig et al., 2015). In the present study, MCLR exposure (30 μg/kg) resulted in increased kidney weights (Control vehicle: 2.71 ± 0.05 g; Control MCLR: 3.01 ± 0.28 g and HFHC vehicle: 2.62 ± 0.17 g; HFHC MCLR: 3.08 ± 0.13 g; mean ± SD) and kidney-to-body weight ratios (Control vehicle: 0.007 ± 0.0003 g; Control MCLR: 0.008 ± 0.0007 g and HFHC vehicle: 0.006 ± 0.0005 g; HFHC MCLR: 0.008 ± 0.0005 g; mean ± SD) despite no change in body weights due to the diet or MCLR toxicity (Arman et al., 2019) (Supplemental Table 1). Pathologist's incidence and severity scoring of H&E stained kidney sections indicated increased overall kidney pathology and glomerular changes in both control and HFHC groups after MCLR exposure (30 μg/kg), with elevated pathology in HFHC diet (Fig. 1 and Fig. 2A-B). Glomerular changes were due to expansion in the mesangial matrix and proliferation of mesangial cells, which are important aspects of diabetic nephropathy (Mason and Wahab, 2003; Schlöndorff and Banas, 2009). Sub-chronic MCLR exposure (30 μg/kg) increased renal tubular protein casts only in the HFHC group (Fig. 2C), suggesting increased susceptibility to MCLR-induced kidney casts in the context of a poor diet. Depending on the nature of the renal intratubular cast, they can be attributed to normal physiology, glomerulonephritis, or other disease states (Dvanajscak et al., 2020). Eosinophilic casts were previously reported in Wistar rats after chronic (8 month) MCLR exposure (Milutinović et al., 2003). There is a lack of substantial change in the other endpoints of kidney health (tubule dilation, necrosis, degeneration) after MCLR exposure (Fig. 2D–E). However, the regeneration score increases after the low dose MCLR exposure in the HFHC group and in both the diet groups after the high dose MCLR (Fig. 2G).

Regeneration is associated with proximal tubule repair after an injury (Fujigaki, 2012). Collectively, these data suggest sub-chronic MCLR exposure causes kidney toxicity in both healthy and HFHC groups, with increased susceptibility to casts in the HFHC group. The glomerular changes, casts and regeneration score suggest MCLR may alter glomerular filtration, protein reabsorption, and/or cause tubule cell damage.

3.2. MCLR kidney toxicity involves proximal tubule cell damage

Proteinuria is a hallmark of CKD (Chacar et al., 2017; Gorriz and Martinez-Castelao, 2012; Mills et al., 2015). MCLR exposure (30 μg/kg) at days 1 and 29 caused proteinuria from 0 to 24 h in the HFHC diet group but caused proteinuria from 0 to 24 h only on day 29 in the control diet group (Fig. 3A, λ symbols). At days 1 and 29 the HFHC diet group exhibited higher proteinuria compared to the control diet group (Fig. 3A, ɵ symbols). These data are consistent with a previous report indicating MCLR exposure in male Wistar rats increased proteinuria (Lowe et al., 2012), although the effect in the present study was more pronounced in the HFHC group. Proteinuria can be caused by glomerular and/or tubulointerstitial damage (Kamijo et al., 2002), so the effects of MCLR and the HFHC diet on glomerular function and tubule cell damage were tested further.

Albuminuria, a common form of proteinuria caused by impaired glomerular filtration and/or albumin reabsorption, was investigated. Urinary albumin levels were not altered by the HFHC diet or MCLR exposure (Fig. 3B). The membrane receptors megalin and cubilin in the proximal tubule cells are responsible for albumin reabsorption in the tubule (Christensen and Birn, 2002, 2001). No changes in renal megalin and cubilin mRNA expression were observed after sub-chronic MCLR exposure in either the control or HFHC diet groups (Fig. 3C and D). These data indicate albumin did not contribute to MCLR-elicited proteinuria and that glomerular filtration may not be involved.

To further assess glomerular function, glomerular filtration rate was estimated using creatinine clearance (Bazzano et al., 2015; Kampmann and Hansen, 1981). Neither the HFHC diet nor sub-chronic MCLR exposure affected creatinine clearance (Fig. 3E), despite histopathology suggesting glomerular changes. Active tubular secretion of creatinine through organic cation transporter 2 (OCT2) and multidrug and toxin extrusion transporter 1 and 2 (MATE1 and MATE2) (Mathialagan et al., 2017; Zhang et al., 2015) accounts for 10–40% of creatinine clearance (Levey et al., 1988; Zhang et al., 2015). MCLR exposure did not alter mRNA expression of OCT2, MATE1 and MATE2 in the control or HFHC groups (Fig. 3F–H), suggesting creatinine tubular secretion was not altered by the HFHC diet or by sub-chronic MCLR exposure. These results are consistent with previous data indicating that short-term high fat diet (6 weeks) did not alter creatinine clearance in Sprague Dawley rats (Crinigan et al., 2015), but are in contrast to another study in male Wistar rats that reported increased creatinine clearance 24 h after a single i.p. injection of 55 μg/kg MCLR (Lowe et al., 2012). The different MCLR effects on creatinine clearance between the current study and Lowe et al. may reflect differences in exposure level/time and/or the strain of rat used. Thus, glomerular filtration did not contribute to MCLR-elicited proteinuria in the current study.

Tubulointerstitial damage was assessed by measuring urinary KIM-1 and THP, two possible non-albumin sources of proteinuria (Fraser et al., 2014; Katayev et al., 2017; Kwon et al., 2019). KIM-1 is a marker of damage and regeneration of renal proximal tubules (Bonventre, 2009; Sabbisetti et al., 2014; Zhang and Cai, 2016), while THP is primarily expressed in the thick ascending loop of Henle and the distal tubule, is responsible for tubular cast formation and tubular obstruction after kidney injury, and is increased in urine of CKD patients (Gorriz and Martinez-Castelao, 2012; Prajczer et al., 2010; Rampoldi et al., 2011; Sikri et al., 1981; Wangsiripaisan et al., 2001). Similar to the proteinuria results, the total 24 h urinary KIM-1 concentration increased only in the HFHC diet group at day 1 (Fig. 4A, day 1, λ symbol). Interestingly, the total 24 h urinary KIM-1 increased only in the control diet group at day 29 (Fig. 4A, day 29, λ symbol), suggesting early damage to proximal tubule cells in the HFHC group and sub-chronic damage in the healthy group. Urinary THP was not altered after sub-chronic MCLR exposure in either control or HFHC diet groups (Fig. 4B). Immunohistochemistry staining of apoptotic markers Bcl-2, Caspase-8, and Bax did not show definitive diet or MCLR effects (Supplemental Figure 1), suggesting that at the time point collected (24 hours after the final MCLR dose) apoptosis was not occurring. Collectively, these data indicate that MCLR-elicited proteinuria may partially reflect proximal tubule cell damage as indicated by increased release of KIM-1.

Excessive urine production (polyuria) is a common symptom of kidney disease and is associated with proteinuria (Fulchiero and Seo-Mayer, 2019; Vieira et al., 2019). MCLR exposure (30 μg/kg) at days 1 and 29 caused polyuria from 0 to 24 h in the control diet group (Fig. 4C, λ symbol), but only caused polyuria from 0 to 6 h after MCLR exposure in the HFHC diet group (Fig. 4C, * symbol). A possible cause of the increased urine production can be attributed to polydipsia, which has been reported previously in mice after MCLR exposure (Zhao et al., 2015), MCLR treatment also increased urine flow in perfused rat kidneys, which would not be affected by water consumption (Nobre et al., 1999). These data indicate MCLR-elicited polyuria may be affected by water consumption and/or renal urine production. Na^+-K^+−2Cl cotransporter 2 (NKCC2), encoded by the solute carrier family 12 member 1 (*Slc12a1*) gene, plays an important role in maintaining body salt and water homeostasis (Ares et al., 2011; Kemter et al., 2010), but sub-chronic MCLR exposure did not alter *Slc12a1* gene expression (Fig. 4D).

The general concordance between KIM-1, polyuria, proteinuria, and renal casts after MCLR exposure suggests that proximal tubule cell damage contributed to these connected pathologies (Larson, 1994; Schentag et al., 1979). Thus, damage to and subsequent regeneration of the proximal tubule cells (Fig. 2G and Fig. 4A) contributed to cast formation (Fig. 2C) and polyuria (Fig. 4C), potentially by affecting the concentrating function of the proximal tubule cells, thin loop of Henle, and the distal tubules. Further research is needed to determine whether tubule cell damage is a result of necrotic or apoptotic cell death and whether the kidney will recover after MCLR toxicity.

3.3. Protein phosphatase expression and inflammation:

The predominant mechanism for MCLR cellular toxicity is covalent binding to the catalytic subunit and inhibition of protein phosphatase 1 and 2A (PP1 and PP2A, respectively),

leading to increased phosphorylation of key proteins involved in signal transduction pathways (Runnegar et al., 1993; Xing et al., 2006; Zong et al., 2018). The effects of MCLR on kidney protein phosphatases have not been explored *in vivo,* although they have been reported for PP2A in human embryonic kidney (HEK) 293 cells (Li et al., 2011). Sub-chronic MCLR exposure (30 μg/kg) decreased PP1 and PP2A protein expression only in the HFHC diet group (Fig. 5A, B, C, E), indicating the HFHC group was more susceptible to MCLR-elicited changes in protein phosphatase expression compared to the healthy group. We previously reported a lower molecular weight PP2A band (~25 kDa) in the liver after sub-chronic MCLR exposure (Arman et al., 2019), and a similar band was observed in the kidney of these animals (Fig. 5D, E). Protein phosphatase-bound MCLR can be measured by western blot using an MCLR specific antibody (Arman et al., 2019; Li et al., 2011). As expected, MCLR bands were observed in the MCLR treated groups (Fig. 5F–H) that correspond to the bands observed for PP2A (37 kDa and 25 kDa). These data show that MCLR reaches the kidney in sufficient amounts to alter protein phosphatase expression in HFHC diet group.

Cytokines play an important role in diet- and/or toxin-induced renal damage. High-fat diets are known to cause renal inflammation (Altunkaynak et al., 2008; Odermatt, 2011) and in the current study the HFHC diet increased proinflammatory *IL-1β* and *Tnf-α* expression (Fig. 6C–D). A previous study reported a concentration-dependent effect of MCLR on IL-1β and Tnf-α production in mouse jejunum, with downregulation occurring at higher MCLR concentrations (Cao et al., 2019). In the current study, *IL-1β* expression decreased after 10 and 30 μg/kg MCLR in the HFHC diet group (Fig. 6C). The role of IL-1β in different types of kidney damage and disease is complicated and may be context-dependent, making it difficult to ascertain the impact of decreased expression on MCLR-elicited renal toxicity in the context of the HFHC diet (Anders, 2016). Increased circulating IL-10 has been reported in diabetic patients and can predict proteinuria in diabetic nephropathy (Sinuani et al., 2013). The role of IL-10 as an attenuator of inflammation and renal fibrosis has also been reported (Jin et al., 2013; Sziksz et al., 2015). Kidney *IL-10* expression increased in the HFHC diet group but decreased to control levels after sub-chronic exposure to both 10 and 30 μg/kg of MCLR (Fig. 6B). The cytokines IL-10 and IL-1β were more sensitive to MCLR as they were the only two molecular endpoints assessed that changed in the kidney after the 10 μg/kg MCLR exposure. It is interesting to note that the HFHC and MCLR effects on *Tnf-α*, *IL-10*, and *IL-1β* were similar in the kidney and liver of these animals (Arman et al., 2019). Another key observation was an increase in the mRNA expression of Vimentin (*Vim*) only in the 30 μg/kg MCLR HFHC group (Fig. 6A). Previous studies have associated vimentin expression with acute and chronic renal tubulointerstitial damage (Fujigaki et al., 2017; Gröne et al., 1987), suggesting the HFHC group was potentially more prone to MCLR-elicited tubulointerstitial toxicity.

3.4. MCLR elimination:

MCLR is detoxified through formation of glutathione and cysteine conjugates (MCLR-GSH and MCLR-Cys, respectively), which are then eliminated in the urine and feces (Gehringer et al., 2004; He et al., 2012; Kondo et al., 1996). Consistent with a previous report (Robinson et al., 1991), a majority of the MCLR excreted into the urine was the parent

molecule (Fig. 7A–C). In addition, our data agree with previous studies indicating parent MCLR is primarily excreted within the first 6 hours after exposure and the MCLR-Cys conjugate is more abundant in the urine compared to MCLR-GSH (Fig. 7A–C) (Ito et al., 2002; Kondo et al., 1996).

The amount of MCLR and its metabolites eliminated in the urine was differential between the diet groups and the exposure time. MCLR-GSH and MCLR-Cys were eliminated in a dose-dependent manner after a single MCLR exposure only in the HFHC group (Fig. 7B–C, day 1, λ symbol), whereas after repeated MCLR exposure they were eliminated in a dose-dependent manner only in the control group (Fig. 7B–C, day 29, λ symbol). The total amount of MCLR-Cys excreted in the urine was higher in both diet groups at day 29 compared to day 1 (Fig. 7C), suggesting the animals adapted to sub-chronic exposure by eliminating more MCLR as the cysteine conjugate. Finally, at day 29 the HFHC group eliminated less MCLR-GSH and MCLR-Cys compared to the control diet group after 30 μg/kg MCLR (Fig. 7B–C, day 29, ɵ symbol). Taken together, these data indicate that the healthy group adapted better to repeated MCLR exposure and eliminated more MCLR through metabolism than the HFHC group.

4. Conclusions:

The connection between MCLR exposure and impaired kidney function was only recently reported in human populations (Lin et al., 2016). The research presented here indicates that MCLR exposure in the context of an HFHC diet may increase the risk of developing renal casts, decrease protein phosphatase expression, dysregulate inflammatory mediators, and decrease MCLR detoxification and urinary excretion. More research is needed to determine whether human populations with obesity and/or NAFLD are at greater risk of MCLR-elicited renal toxicities.

Supplementary Material

Refer to Web version on PubMed Central for supplementary material.

Acknowledgement

The authors gratefully acknowledge Dr. Allen J. Baron for his expert comments and advice during the writing of the paper. The author also acknowledges the financial support by the National Institute of Environmental Health Sciences [grant number K99/R00ES024455] and Washington State University.

Abbreviations:

MCLR	Microcystin-LR
NAFLD	Non-alcoholic fatty liver disease
CKD	Chronic kidney disease
HFHC	High fat/high cholesterol
PP1/2A	Protein phosphatase 1/2A

Tnf-α	Tumor necrosis factor-alpha
IL-10	Interleukin-10
L-1β	Interleukin- 1 beta
Slc47a1/2	Solute Carrier Family 47 Member 1/2
Slc12a1	Solute Carrier Family 12 member 1
Lrp2	LDL Receptor related Protein 2
Slc22a2	Solute carrier family 22 member 2
Mate1/2	Multidrug and toxin extrusion transporter 1/2
OCT2	Organic cation transporter 2 (OCT2)
NKCC2	Na^+-K^+-2Cl cotransporter 2
THP	Tamm-Horsfall protein
KIM-1	Kidney injury molecule 1
MCLR-GSH	MCLR-glutathione
MCLR-Cys	MCLR-cysteine

References:

Abdel-Daim MM, Sayed AA, Abdeen A, Aleya L, Ali D, Alkahtane AA, Alarifi S, Alkahtani S, 2019. Piperine enhances the antioxidant and anti-inflammatory activities of thymoquinone against microcystin-LR-induced hepatotoxicity and neurotoxicity in mice. Oxid. Med. Cell. Longev 2019. 10.1155/2019/1309175

Aldridge GM, Podrebarac DM, Greenough WT, Weiler IJ, 2008. The use of total protein stains as loading controls: an alternative to high-abundance single-protein controls in semi-quantitative immunoblotting. J. Neurosci. Methods 172, 250–4. 10.1016/j.jneumeth.2008.05.003 [PubMed: 18571732]

AlKahtane AA, Abushouk AI, Mohammed ET, ALNasser M, Alarifi S, Ali D, Alessia MS, Almeer RS, AlBasher G, Alkahtani S, Aleya L, Abdel-Daim MM, 2020. Fucoidan alleviates microcystin-LR-induced hepatic, renal, and cardiac oxidative stress and inflammatory injuries in mice. Environ. Sci. Pollut. Res 27, 2935–2944. 10.1007/s11356-019-06931-z

Altunkaynak ME, Özbek E, Altunkaynak BZ, Can İ, Unal D, Unal B, 2008. The effects of high-fat diet on the renal structure and morphometric parametric of kidneys in rats. J. Anat 212, 845–852. 10.1111/j.1469-7580.2008.00902.x [PubMed: 18510511]

Anders H-J, 2016. Of Inflammasomes and Alarmins: IL-1β and IL-1α in Kidney Disease. J. Am. Soc. Nephrol 27, 2564–75. 10.1681/ASN.2016020177 [PubMed: 27516236]

Ares GR, Caceres PS, Ortiz PA, 2011. Molecular regulation of NKCC2 in the thick ascending limb. Am. J. Physiol. Physiol 301, F1143–F1159. 10.1152/ajprenal.00396.2011

Arman T, Lynch KD, Montonye ML, Goedken M, Clarke JD, 2019. Sub-Chronic Microcystin-LR Liver Toxicity in Preexisting Diet-Induced Nonalcoholic Steatohepatitis in Rats. Toxins (Basel). 11, 398. 10.3390/toxins11070398

Bazzano T, Restel TI, Porfirio LC, de Souza AS, Silva IS, 2015. Renal biomarkers of male and female Wistar rats (Rattus norvegicus) undergoing renal ischemia and reperfusion. Acta Cir. Bras 30, 277–288. 10.1590/S0102-865020150040000007 [PubMed: 25923261]

Bonventre JV, 2009. Kidney injury molecule-1 (KIM-1): a urinary biomarker and much more. Nephrol. Dial. Transplant 24, 3265–8. 10.1093/ndt/gfp010 [PubMed: 19318357]

Campos A, Vasconcelos V, 2010. Molecular mechanisms of microcystin toxicity in animal cells. Int. J. Mol. Sci 11, 268–87. 10.3390/ijms11010268 [PubMed: 20162015]

Cao L, Huang F, Massey IY, Wen C, Zheng S, Xu S, Yang F, 2019. Effects of Microcystin-LR on the Microstructure and Inflammation-Related Factors of Jejunum in Mice. Toxins (Basel). 11, 482. 10.3390/toxins11090482

Chacar F, Kogika M, Sanches TR, Caragelasco D, Martorelli C, Rodrigues C, Capcha JMC, Chew D, Andrade L, 2017. Urinary Tamm-Horsfall protein, albumin, vitamin D-binding protein, and retinol-binding protein as early biomarkers of chronic kidney disease in dogs. Physiol. Rep 5, e13262. 10.14814/phy2.13262

Christensen EI, Birn H, 2002. Megalin and cubilin: multifunctional endocytic receptors. Nat. Rev. Mol. Cell Biol 3, 258–267. 10.1038/nrm778

Christensen EI, Birn H, 2001. Megalin and cubilin: synergistic endocytic receptors in renal proximal tubule. Am. J. Physiol. Physiol 280, F562–F573. 10.1152/ajprenal.2001.280.4.F562

Clarke JD, Dzierlenga A, Arman T, Toth E, Li H, Lynch KD, Tian D-D, Goedken M, Paine MF, Cherrington N, 2019. Nonalcoholic fatty liver disease alters microcystin-LR toxicokinetics and acute toxicity. Toxicon 162, 1–8. 10.1016/j.toxicon.2019.03.002 [PubMed: 30849452]

Coresh J, 2017. Update on the Burden of CKD. J. Am. Soc. Nephrol 28, 1020–1022. 10.1681/ASN.2016121374 [PubMed: 28302756]

Craig EA, Yan Z, Zhao QJ, 2015. The relationship between chemical-induced kidney weight increases and kidney histopathology in rats. J. Appl. Toxicol 35, 729–736. 10.1002/jat.3036 [PubMed: 25092041]

Crinigan C, Calhoun M, Sweazea KL, 2015. Short-Term High Fat Intake Does Not Significantly Alter Markers of Renal Function or Inflammation in Young Male Sprague-Dawley Rats. J. Nutr. Metab 2015, 1–9. 10.1155/2015/157520

Dvanajscak Z, Cossey LN, Larsen CP, 2020. A practical approach to the pathology of renal intratubular casts. Semin. Diagn. Pathol 37, 127–134. 10.1053/j.semdp.2020.02.001 [PubMed: 32147230]

Fawell JK, Mitchell RE, Everett DJ, Hill RE, 1999. The toxicity of cyanobacterial toxins in the mouse: I Microcystin-LR. Hum. Exp. Toxicol 18, 162–167. 10.1177/096032719901800305 [PubMed: 10215106]

Fischer A, Hoeger SJ, Stemmer K, Feurstein DJ, Knobeloch D, Nussler A, Dietrich DR, 2010. The role of organic anion transporting polypeptides (OATPs/SLCOs) in the toxicity of different microcystin congeners in vitro: A comparison of primary human hepatocytes and OATP-transfected HEK293 cells. Toxicol. Appl. Pharmacol 245, 9–20. 10.1016/j.taap.2010.02.006 [PubMed: 20171238]

Fischer WJ, Altheimer S, Cattori V, Meier PJ, Dietrich DR, Hagenbuch B, 2005. Organic anion transporting polypeptides expressed in liver and brain mediate uptake of microcystin. Toxicol.Appl.Pharmacol 203, 257–263. 10.1016/j.taap.2004.08.012 [PubMed: 15737679]

Fraser SDS, Roderick PJ, McIntyre NJ, Harris S, McIntyre C, Fluck R, Taal MW, 2014. Assessment of Proteinuria in Patients with Chronic Kidney Disease Stage 3: Albuminuria and Non-Albumin Proteinuria. PLoS One 9, e98261. 10.1371/journal.pone.0098261

Fujigaki Y, 2012. Different modes of renal proximal tubule regeneration in health and disease. World J. Nephrol 1, 92. 10.5527/wjn.v1.i4.92 [PubMed: 24175246]

Fujigaki Y, Tamura Y, Nagura M, Arai S, Ota T, Shibata S, Kondo F, Yamaguchi Y, Uchida S, 2017. Unique proximal tubular cell injury and the development of acute kidney injury in adult patients with minimal change nephrotic syndrome. BMC Nephrol. 18, 339. 10.1186/s12882-017-0756-6 [PubMed: 29179690]

Fulchiero R, Seo-Mayer P, 2019. Bartter Syndrome and Gitelman Syndrome. Pediatr. Clin. North Am 66, 121–134. 10.1016/j.pcl.2018.08.010 [PubMed: 30454738]

Gehringer MM, Shephard EG, Downing TG, Wiegand C, Neilan BA, 2004. An investigation into the detoxification of microcystin-LR by the glutathione pathway in Balb/c mice. Int.J Biochem. Biol. 36, 931–941. 10.1016/j.biocel.2003.10.012

Gorriz JL, Martinez-Castelao A, 2012. Proteinuria: detection and role in native renal disease progression. Transplant. Rev 26, 3–13. 10.1016/j.trre.2011.10.002

Gröne HJ, Weber K, Gröne E, Helmchen U, Osborn M, 1987. Coexpression of keratin and vimentin in damaged and regenerating tubular epithelia of the kidney. Am. J. Pathol 129, 1–8. [PubMed: 2444108]

He J, Chen J, Xie P, Zhang D, Li G, Wu L, Zhang W, Guo X, Li S, 2012. Quantitatively evaluating detoxification of the hepatotoxic microcystins through the glutathione and cysteine pathway in the cyanobacteria-eating bighead carp. Aquat.Toxicol 116–117, 61–68. 10.1016/j.aquatox.2012.03.004

Hill NR, Fatoba ST, Oke JL, Hirst JA, O'Callaghan CA, Lasserson DS, Hobbs FDR, 2016. Global Prevalence of Chronic Kidney Disease – A Systematic Review and Meta-Analysis. PLoS One 11, e0158765. 10.1371/journal.pone.0158765

Ibrahim SH, Hirsova P, Malhi H, Gores GJ, 2016. Animal Models of Nonalcoholic Steatohepatitis: Eat, Delete, and Inflame. Dig. Dis. Sci 61, 1325–1336. 10.1007/s10620-015-3977-1 [PubMed: 26626909]

Ito E, Takai A, Kondo F, Masui H, Imanishi S, Harada K-I, 2002. Comparison of protein phosphatase inhibitory activity and apparent toxicity of microcystins and related compounds. Toxicon 40, 1017–1025. 10.1016/S0041-0101(02)00099-5 [PubMed: 12076656]

Jin Y, Liu R, Xie J, Xiong H, He JC, Chen N, 2013. Interleukin-10 deficiency aggravates kidney inflammation and fibrosis in the unilateral ureteral obstruction mouse model. Lab. Investig 93, 801–811. 10.1038/labinvest.2013.64 [PubMed: 23628901]

Kamijo A, Kimura K, Sugaya T, Yamanouchi M, Hase H, Kaneko T, Hirata Y, Goto A, Fujita T, Omata M, 2002. Urinary free fatty acids bound to albumin aggravate tubulointerstitial damage. Kidney Int. 62, 1628–37. 10.1046/j.1523-1755.2002.00618.x [PubMed: 12371963]

Kampmann J, Hansen J, 1981. Glomerular filtration rate and creatinine clearance. Br. J. Clin. Pharmacol 12, 7–14. 10.1111/j.1365-2125.1981.tb01848.x [PubMed: 6788057]

Kataria A, Trasande L, Trachtman H, 2015. The effects of environmental chemicals on renal function. Nat. Rev. Nephrol 11, 610–625. 10.1038/nrneph.2015.94 [PubMed: 26100504]

Katayev A, Zebelman AM, Sharp TM, Samantha Flynn, Bernstein RK, 2017. Prevalence of isolated non-albumin proteinuria in the US population tested for both, urine total protein and urine albumin: An unexpected discovery. Clin. Biochem 50, 262–269. 10.1016/j.clinbiochem.2016.11.030 [PubMed: 27916507]

Kemter E, Rathkolb B, Bankir L, Schrewe A, Hans W, Landbrecht C, Klaften M, Ivandic B, Fuchs H, Gailus-Durner V, Hrabé de Angelis M, Wolf E, Wanke R, Aigner B, 2010. Mutation of the Na + -K + −2Cl − cotransporter NKCC2 in mice is associated with severe polyuria and a urea-selective concentrating defect without hyperreninemia. Am. J. Physiol. Physiol 298, F1405–F1415. 10.1152/ajprenal.00522.2009

Kondo F, Matsumoto H, Yamada S, Ishikawa N, Ito E, Nagata S, Ueno Y, Suzuki M, Harada K, 1996. Detection and identification of metabolites of microcystins formed in vivo in mouse and rat livers. Chem.Res.Toxicol 9, 1355–1359. 10.1021/tx960085a [PubMed: 8951240]

Kramer H, Luke A, 2007. Obesity and kidney disease: a big dilemma. Curr. Opin. Nephrol. Hypertens 16, 237–41. 10.1097/MNH.0b013e32803578e4 [PubMed: 17420667]

Kwon OC, Park Y, Lee JS, Oh JS, Kim Y-G, Lee C-K, Yoo B, Hong S, 2019. Non-albumin proteinuria as a parameter of tubulointerstitial inflammation in lupus nephritis. Clin. Rheumatol 38, 235–241. 10.1007/s10067-018-4256-2 [PubMed: 30094751]

Larson TS, 1994. Evaluation of Proteinuria. Mayo Clin. Proc 69, 1154–1158. 10.1016/S0025-6196(12)65767-X [PubMed: 7967776]

Laurentius T, Raffetseder U, Fellner C, Kob R, Nourbakhsh M, Floege J, Bertsch T, Bollheimer LC, Ostendorf T, 2019. High-fat diet-induced obesity causes an inflammatory microenvironment in the kidneys of aging Long-Evans rats. J. Inflamm 16, 14. 10.1186/s12950-019-0219-x

Levey AS, Atkins R, Coresh J, Cohen EP, Collins AJ, Eckardt K-U, Nahas ME, Jaber BL, Jadoul M, Levin A, Powe NR, Rossert J, Wheeler DC, Lameire N, Eknoyan G, 2007. Chronic kidney disease as a global public health problem: Approaches and initiatives – a position statement from Kidney Disease Improving Global Outcomes. Kidney Int. 72, 247–259. 10.1038/sj.ki.5002343 [PubMed: 17568785]

Levey AS, Perrone RD, Madias NE, 1988. Serum Creatinine and Renal Function. Annu. Rev. Med 39, 465–490. 10.1146/annurev.me.39.020188.002341 [PubMed: 3285786]

Li T, Huang P, Liang J, Fu W, Guo Z-L, Xu L-H, 2011. Microcystin-LR (MCLR) induces a compensation of PP2A activity mediated by α4 protein in HEK293 cells. Int. J. Biol. Sci 7, 740–52. 10.7150/ijbs.7.740

Liang J, Li T, Zhang Y-L, Guo Z-L, Xu L-H, 2011. Effect of microcystin-LR on protein phosphatase 2A and its function in human amniotic epithelial cells. J. Zhejiang Univ. Sci. B 12, 951–60. 10.1631/jzus.B1100121 [PubMed: 22135143]

Lin H, Liu W, Zeng H, Pu C, Zhang R, Qiu Z, Chen J-A, Wang L, Tan Y, Zheng C, Yang X, Tian Y, Huang Y, Luo J, Luo Y, Feng X, Xiao G, Feng L, Li H, Wang F, Yuan C, Wang J, Zhou Z, Wei T, Zuo Y, Wu L, He L, Guo Y, Shu W, 2016. Determination of Environmental Exposure to Microcystin and Aflatoxin as a Risk for Renal Function Based on 5493 Rural People in Southwest China. Environ. Sci. Technol 50, 5346–5356. 10.1021/acs.est.6b01062 [PubMed: 27071036]

Liu J, Sun Y, 2015. The role of PP2A-associated proteins and signal pathways in microcystin-LR toxicity. Toxicol. Lett 236, 1–7. 10.1016/j.toxlet.2015.04.010 [PubMed: 25922137]

Lowe J, Souza-Menezes J, Freire DS, Mattos LJ, Castiglione RC, Barbosa CML, Santiago L, Ferrão FM, Cardoso LHD, da Silva RT, Vieira-Beiral HJ, Vieyra A, Morales MM, Azevedo SMFO, Soares RM, 2012. Single sublethal dose of microcystin-LR is responsible for different alterations in biochemical, histological and physiological renal parameters. Toxicon 59, 601–609. 10.1016/j.toxicon.2012.02.003 [PubMed: 22387752]

Mason RM, Wahab NA, 2003. Extracellular matrix metabolism in diabetic nephropathy. J. Am. Soc. Nephrol 14, 1358–73. 10.1097/01.asn.0000065640.77499.d7 [PubMed: 12707406]

Mathialagan S, Rodrigues AD, Feng B, 2017. Evaluation of Renal Transporter Inhibition Using Creatinine as a Substrate In Vitro to Assess the Clinical Risk of Elevated Serum Creatinine. J. Pharm. Sci 106, 2535–2541. 10.1016/j.xphs.2017.04.009 [PubMed: 28416419]

Michael B, Yano B, Sellers RS, Perry R, Morton D, Roome N, Johnson JK, Schafer K, 2007. Evaluation of Organ Weights for Rodent and Non-Rodent Toxicity Studies: A Review of Regulatory Guidelines and a Survey of Current Practices. Toxicol. Pathol 35, 742–750. 10.1080/01926230701595292 [PubMed: 17849357]

Mills KT, Xu Y, Zhang W, Bundy JD, Chen C-S, Kelly TN, Chen J, He J, 2015. A systematic analysis of worldwide population-based data on the global burden of chronic kidney disease in 2010. Kidney Int. 88, 950–957. 10.1038/ki.2015.230 [PubMed: 26221752]

Milutinović A, Zivin M, Zorc-Pleskovic R, Sedmak B, Suput D, Milutinovic A, Zivin M, Zorc-Pleskovic R, Sedmak B, Suput D, 2003. Nephrotoxic effects of chronic administration of microcystins -LR and -YR. Toxicon 42, 281–288. 10.1016/S0041-0101(03)00143-0 [PubMed: 14559079]

Montonye ML, Tian D-D, Arman T, Lynch KD, Hagenbuch B, Paine MF, Clarke JD, 2019. A Pharmacokinetic Natural Product-Disease-Drug Interaction: A Double Hit of Silymarin and Nonalcoholic Steatohepatitis on Hepatic Transporters in a Rat Model. J. Pharmacol. Exp. Ther 371, 385–393. 10.1124/jpet.119.260489 [PubMed: 31420525]

More SS, Akil O, Ianculescu AG, Geier EG, Lustig LR, Giacomini KM, 2010. Role of the Copper Transporter, CTR1, in Platinum-Induced Ototoxicity. J. Neurosci 30, 9500–9509. 10.1523/JNEUROSCI.1544-10.2010 [PubMed: 20631178]

Musso G, Gambino R, Tabibian JH, Ekstedt M, Kechagias S, Hamaguchi M, Hultcrantz R, Hagström H, Yoon SK, Charatcharoenwitthaya P, George J, Barrera F, Haflidadóttir S, Björnsson ES, Armstrong MJ, Hopkins LJ, Gao X, Francque S, Verrijken A, Yilmaz Y, Lindor KD, Charlton M, Haring R, Lerch MM, Rettig R, Völzke H, Ryu S, Li G, Wong LL, Machado M, Cortez-Pinto H, Yasui K, Cassader M, 2014. Association of Non-alcoholic Fatty Liver Disease with Chronic Kidney Disease: A Systematic Review and Meta-analysis. PLoS Med. 11. 10.1371/journal.pmed.1001680

Nobre AC, Coelho GR, Coutinho MC, Silva MM, Angelim EV, Menezes DB, Fonteles MC, Monteiro HS, Coêlho GR, Coutinho MC, Silva MM, Angelim EV, Menezes DB, Fonteles MC, Monteiro HS, 2001. The role of phospholipase A(2) and cyclooxygenase in renal toxicity induced by microcystin-LR. Toxicon 39, 721–724. 10.1016/S0041-0101(00)00193-8 [PubMed: 11072052]

Nobre ACL, Jorge MCM, Menezes DB, Fonteles MC, Monteiro HSA, 1999. Effects of microcystin-LR in isolated perfused rat kidney. Brazilian J. Med. Biol. Res 32, 985–988. 10.1590/S0100-879X1999000800008

Odermatt A, 2011. The Western-style diet: a major risk factor for impaired kidney function and chronic kidney disease. Am. J. Physiol. Physiol 301, F919–F931. 10.1152/ajprenal.00068.2011

Paerl HW, Paul VJ, 2012. Climate change: Links to global expansion of harmful cyanobacteria. Water Res. 46, 1349–1363. 10.1016/j.watres.2011.08.002 [PubMed: 21893330]

Prajczer S, Heidenreich U, Pfaller W, Kotanko P, Lhotta K, Jennings P, 2010. Evidence for a role of uromodulin in chronic kidney disease progression. Nephrol. Dial. Transplant 25, 1896–1903. 10.1093/ndt/gfp748 [PubMed: 20075439]

Rampoldi L, Scolari F, Amoroso A, Ghiggeri G, Devuyst O, 2011. The rediscovery of uromodulin (Tamm–Horsfall protein): from tubulointerstitial nephropathy to chronic kidney disease. Kidney Int. 80, 338–347. 10.1038/ki.2011.134 [PubMed: 21654721]

Robinson NA, Pace JG, Matson CF, Miura GA, Lawrence WB, 1991. Tissue distribution, excretion and hepatic biotransformation of microcystin-LR in mice. J Pharmacol.Exp.Ther 256, 176–182. [PubMed: 1988656]

Runnegar MT, Kong S, Berndt N, 1993. Protein phosphatase inhibition and in vivo hepatotoxicity of microcystins. Am. J. Physiol 265, G224–30. 10.1152/ajpgi.1993.265.2.G224 [PubMed: 8396333]

Sabbisetti VS, Waikar SS, Antoine DJ, Smiles A, Wang C, Ravisankar A, Ito K, Sharma S, Ramadesikan S, Lee M, Briskin R, De Jager PL, Ngo TT, Radlinski M, Dear JW, Park KB, Betensky R, Krolewski AS, Bonventre JV, 2014. Blood Kidney Injury Molecule-1 Is a Biomarker of Acute and Chronic Kidney Injury and Predicts Progression to ESRD in Type I Diabetes. J. Am. Soc. Nephrol 25, 2177–2186. 10.1681/ASN.2013070758 [PubMed: 24904085]

Schentag JJ, Gengo FM, Plaut ME, Danner D, Mangione A, Jusko WJ, 1979. Urinary casts as an indicator of renal tubular damage in patients receiving aminoglycosides. Antimicrob. Agents Chemother 16, 468–474. 10.1128/AAC.16.4.468 [PubMed: 518076]

Schlöndorff D, Banas B, 2009. The Mesangial Cell Revisited: No Cell Is an Island. J. Am. Soc. Nephrol 20, 1179–1187. 10.1681/ASN.2008050549 [PubMed: 19470685]

Sikri KL, Foster CL, MacHugh N, Marshall RD, 1981. Localization of Tamm-Horsfall glycoprotein in the human kidney using immuno-fluorescence and immuno-electron microscopical techniques. J. Anat 132, 597–605. [PubMed: 7028707]

Sinn DH, Kang D, Jang HR, Gu S, Cho SJ, Paik SW, Ryu S, Chang Y, Lazo M, Guallar E, Cho J, Gwak G-Y, 2017. Development of chronic kidney disease in patients with non-alcoholic fatty liver disease: A cohort study. J. Hepatol 67, 1274–1280. 10.1016/j.jhep.2017.08.024 [PubMed: 28870674]

Sinuani I, Beberashvili I, Averbukh Z, Sandbank J, 2013. Role of IL-10 in the progression of kidney disease. World J. Transplant 3, 91. 10.5500/wjt.v3.i4.91 [PubMed: 24392313]

Soderland P, Lovekar S, Weiner DE, Brooks DR, Kaufman JS, 2010. Chronic Kidney Disease Associated With Environmental Toxins and Exposures. Adv. Chronic Kidney Dis 17, 254–264. 10.1053/j.ackd.2010.03.011 [PubMed: 20439094]

Svirčev Z, Drobac D, Tokodi N, Mijović B, Codd GA, Meriluoto J, 2017. Toxicology of microcystins with reference to cases of human intoxications and epidemiological investigations of exposures to cyanobacteria and cyanotoxins. Arch. Toxicol 91, 621–650. 10.1007/s00204-016-1921-6 [PubMed: 28042640]

Sziksz E, Pap D, Lippai R, Béres NJ, Fekete A, Szabó AJ, Vannay Á, 2015. Fibrosis Related Inflammatory Mediators: Role of the IL-10 Cytokine Family. Mediators Inflamm. 2015, 1–15. 10.1155/2015/764641

Targher G, Bertolini L, Rodella S, Zoppini G, Lippi G, Day C, Muggeo M, 2008. Non-alcoholic fatty liver disease is independently associated with an increased prevalence of chronic kidney disease and proliferative/laser-treated retinopathy in type 2 diabetic patients. Diabetologia 51, 444–450. 10.1007/s00125-007-0897-4 [PubMed: 18058083]

Targher G, Byrne CD, 2017. Non-alcoholic fatty liver disease: an emerging driving force in chronic kidney disease. Nat. Rev. Nephrol 13, 297–310. 10.1038/nrneph.2017.16 [PubMed: 28218263]

Targher G, Chonchol M, Zoppini G, Abaterusso C, Bonora E, 2011. Risk of chronic kidney disease in patients with non-alcoholic fatty liver disease: is there a link? J Hepatol. 54, 1020–1029. 10.1016/j.jhep.2010.11.007 [PubMed: 21145850]

Vieira Souto, Sánchez-López Machado, Severino Jose, Santini Silva, Fortuna García, Souto, 2019. Sugar-Lowering Drugs for Type 2 Diabetes Mellitus and Metabolic Syndrome—Strategies for In Vivo Administration: Part-II. J. Clin. Med 8, 1332. 10.3390/jcm8091332

Wahlang B, Falkner KC, Gregory B, Ansert D, Young D, Conklin DJ, Bhatnagar A, McClain CJ, Cave M, 2013. Polychlorinated biphenyl 153 is a diet-dependent obesogen that worsens nonalcoholic fatty liver disease in male C57BL6/J mice. J. Nutr. Biochem 24, 1587–95. 10.1016/j.jnutbio.2013.01.009 [PubMed: 23618531]

Wahlang B, Song M, Beier JI, Cameron Falkner K, Al-Eryani L, Clair HB, Prough RA, Osborne TS, Malarkey DE, Christopher States J, Cave MC, 2014. Evaluation of Aroclor 1260 exposure in a mouse model of diet-induced obesity and non-alcoholic fatty liver disease. Toxicol. Appl. Pharmacol 279, 380–390. 10.1016/j.taap.2014.06.019 [PubMed: 24998970]

Wangsiripaisan A, Gengaro PE, Edelstein CL, Schrier RW, 2001. Role of polymeric Tamm-Horsfall protein in cast formation: Oligosaccharide and tubular fluid ions. Kidney Int. 59, 932–940. 10.1046/j.1523-1755.2001.059003932.x [PubMed: 11231348]

Webster AC, Nagler EV, Morton RL, Masson P, 2017. Chronic Kidney Disease. Lancet 389, 1238–1252. 10.1016/S0140-6736(16)32064-5 [PubMed: 27887750]

Xing Y, Xu Y, Chen Y, Jeffrey PD, Chao Y, Lin Z, Li Z, Strack S, Stock JB, Shi Y, 2006. Structure of Protein Phosphatase 2A Core Enzyme Bound to Tumor-Inducing Toxins. Cell 127, 341–353. 10.1016/j.cell.2006.09.025 [PubMed: 17055435]

Yi X, Xu S, Huang F, Wen C, Zheng S, Feng H, Guo J, Chen J, Feng X, Yang F, 2019. Effects of Chronic Exposure to Microcystin-LR on Kidney in Mice. Int. J. Environ. Res. Public Health 16, 5030. 10.3390/ijerph16245030

Zhang Y, Warren MS, Zhang X, Diamond S, Williams B, Punwani N, Huang J, Huang Y, Yeleswaram S, 2015. Impact on Creatinine Renal Clearance by the Interplay of Multiple Renal Transporters: A Case Study with INCB039110. Drug Metab. Dispos 43, 485–489. 10.1124/dmd.114.060673 [PubMed: 25605813]

Zhang Z, Cai CX, 2016. Kidney injury molecule-1 (KIM-1) mediates renal epithelial cell repair via ERK MAPK signaling pathway. Mol. Cell. Biochem 416, 109–116. 10.1007/s11010-016-2700-7 [PubMed: 27084535]

Zhao Y, Xue Q, Su X, Xie L, Yan Y, Steinman AD, 2015. Microcystin-LR induced thyroid dysfunction and metabolic disorders in mice. Toxicology 328, 135–141. 10.1016/j.tox.2014.12.007 [PubMed: 25497113]

Zong W-S, Zhang S-H, Wang Q, Teng Y, Liu Y-Z, Du Y-G, 2018. Evaluation of the Direct and Indirect Regulation Pathways of Glutathione Target to the Hepatotoxicity of Microcystin-LR. Biomed Res. Int 2018, 1–8. 10.1155/2018/5672637

HIGHLIGHTS:

- HFHC diet increased severity of MCLR induced casts and proteinuria
- Urinary KIM-1 levels increased after MCLR exposure
- PP1 and PP2A protein levels decreased after MCLR exposure only in the HFHC group
- HFHC diet decreased the metabolism and total urinary elimination of MCLR

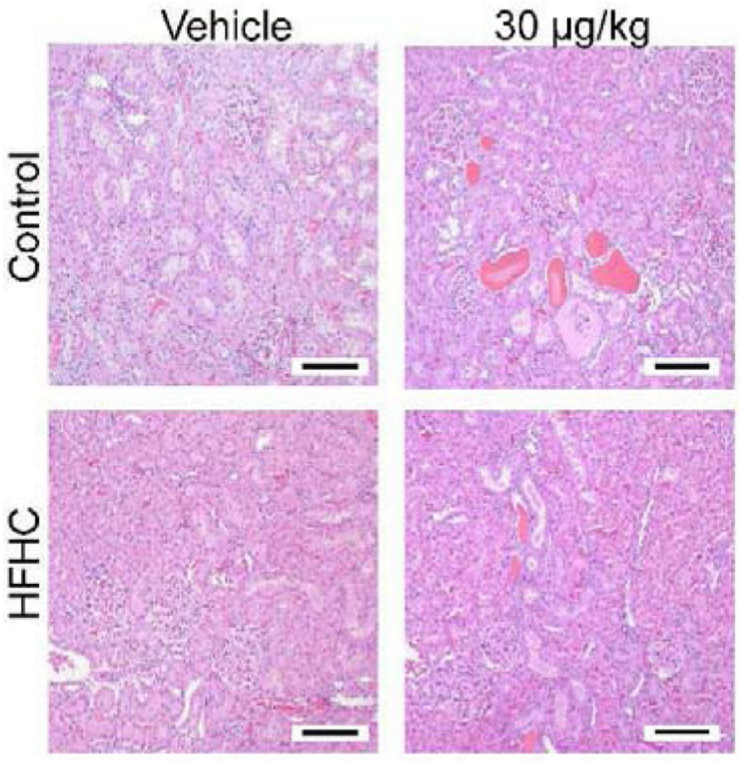

Figure 1:
Representative H&E stained kidneys (Magnification 100X). Size bars represent 100 µm.

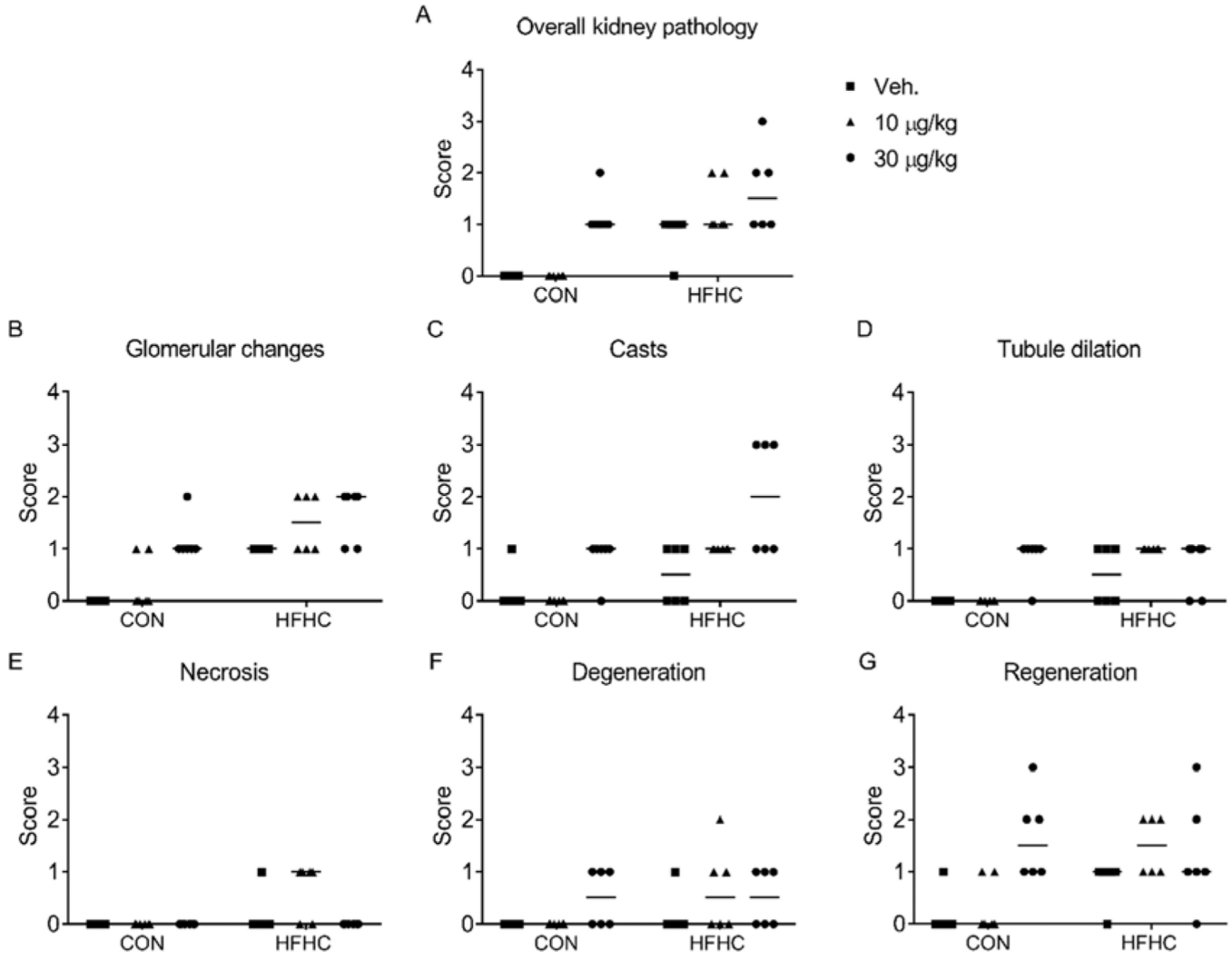

Figure 2:

Histology severity scores. (A) Overall kidney pathology, (B) Glomerular changes, (C) Casts, (D) Tubule dilation, (E) Necrosis, (F) Degeneration, and (G) Regeneration scores provided by the pathologist. Each point represents an individual animal in the group, n=6 per group. The horizontal lines represent the median for each group.

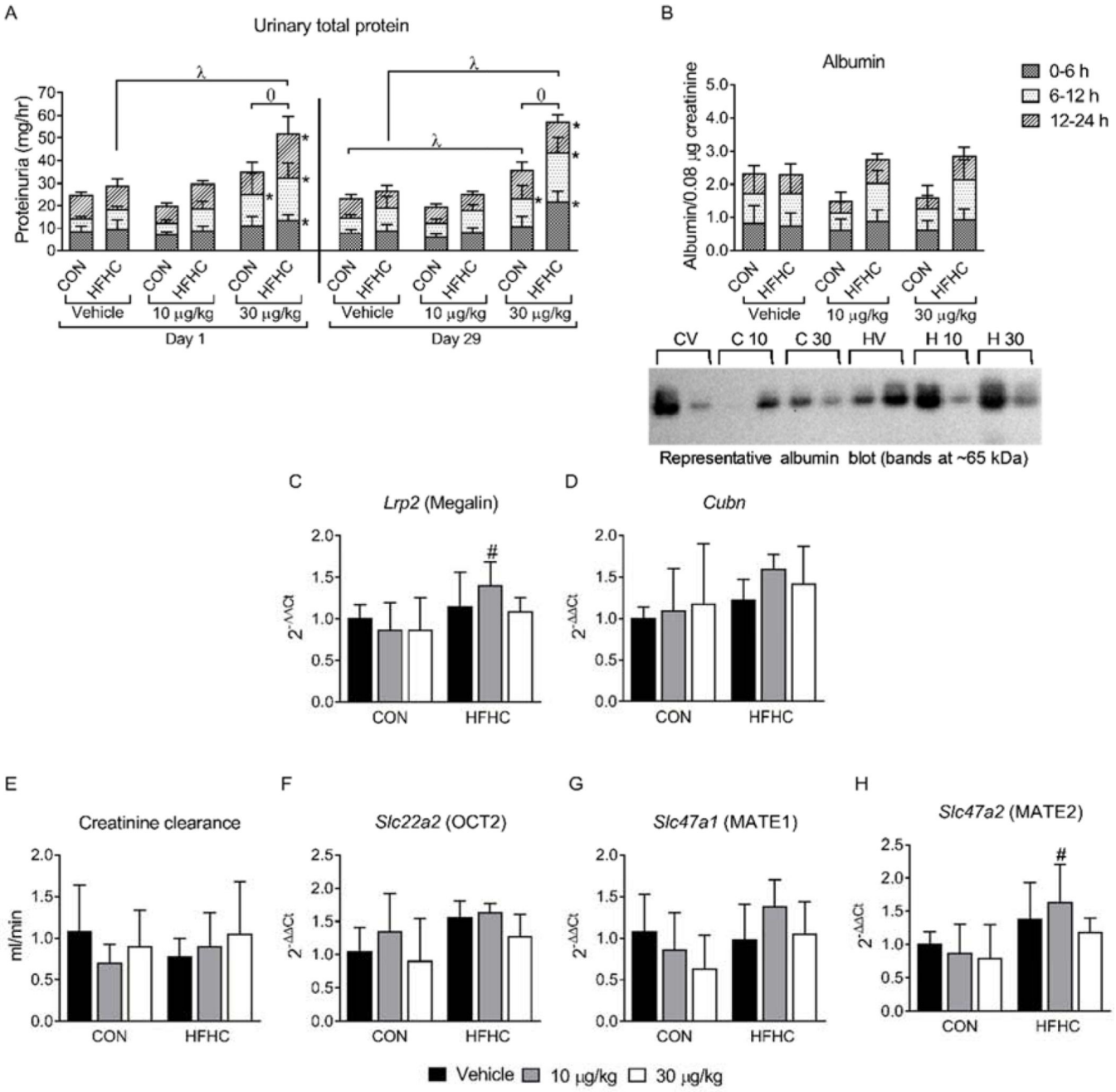

Figure 3:

Proteinuria and Creatinine clearance. (A) Urinary total protein after a single dose (Day 1) and after the final dose of MCLR (Day 29) divided into the urine collection time points (0–6, 6–12, 12–24 h). (B) Densitometry of Day 29 urine albumin divided into the urine collection time points (0–6, 6–12, 12–24 h), along with representative western blots. (C) *Lrp2* (Megalin) and (D) *Cubn* (Cubilin) mRNA expression. (E) Day 29 creatinine clearance. (F) *Slc22a2* (OCT2) (G) *Slc47a1* (MATE1) and (H) *Slc47a2* (MATE2) mRNA expression in the kidney. Data represent mean ± SD, n = 6 per group. Two-way ANOVA Dunnett multiple comparison post-test represented by * indicate p-value <0.05, *versus* respective vehicle

group for each collection period (0–6, 6–12, or 12–24 h). Two-way ANOVA Dunnett multiple comparison post-test represented by (λ) indicate p-value < 0.05 *versus* respective vehicle group for the complete 24-h period. Two-way ANOVA Sidak multiple comparison post-test represented with (ɵ) indicate p-value < 0.05 comparing control *versus* HFHC within each dose for the complete 24-h period. Two-way ANOVA Sidak multiple comparison post-test represented with (#) indicate p-value < 0.05 within each dose group.

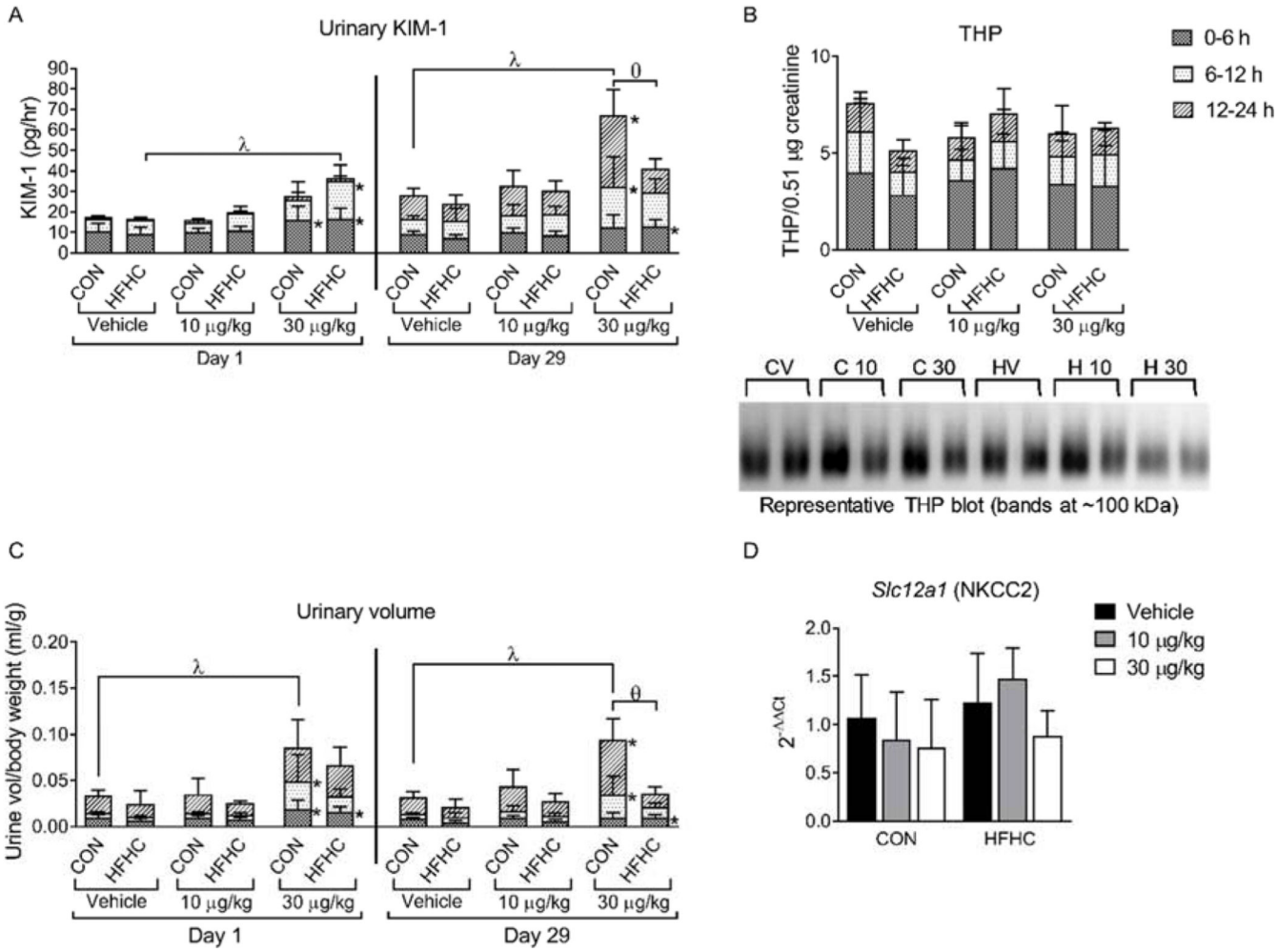

Figure 4:

KIM-1, THP and Polyuria. (A) (F) Urinary KIM-1 after a single dose (Day 1) and after the final dose of MCLR (Day 29) divided into the urine collection time points (0–6, 6–12, 12–24 h). (B) Day 29 urine THP divided into the urine collection time points (0–6, 6–12, 12–24 h), along with representative western blots.(C) Urine volumes after a single dose of MCLR (Day 1) and after the final dose of MCLR (Day 29) divided into the urine collection time points (0 to 6, 6 to 12, 12 to 24 h). (D) *Slc12a1* (NKCC2) mRNA expression in the kidney. (C). Data represent mean ± SD, n = 6 per group. Two-way ANOVA Dunnett multiple comparison post-test represented by * indicate p-value <0.05, *versus* respective vehicle group for each collection period (0 to 6, 6 to 12, or 12 to 24 h). Two-way ANOVA Dunnett multiple comparison post-test represented by (λ) indicate p-value < 0.05 *versus* respective vehicle group for the complete 24-h period. Two-way ANOVA Sidak multiple comparison post-test represented with (ɵ) indicate p-value < 0.05 comparing control *versus* HFHC within each dose for the complete 24-h period.

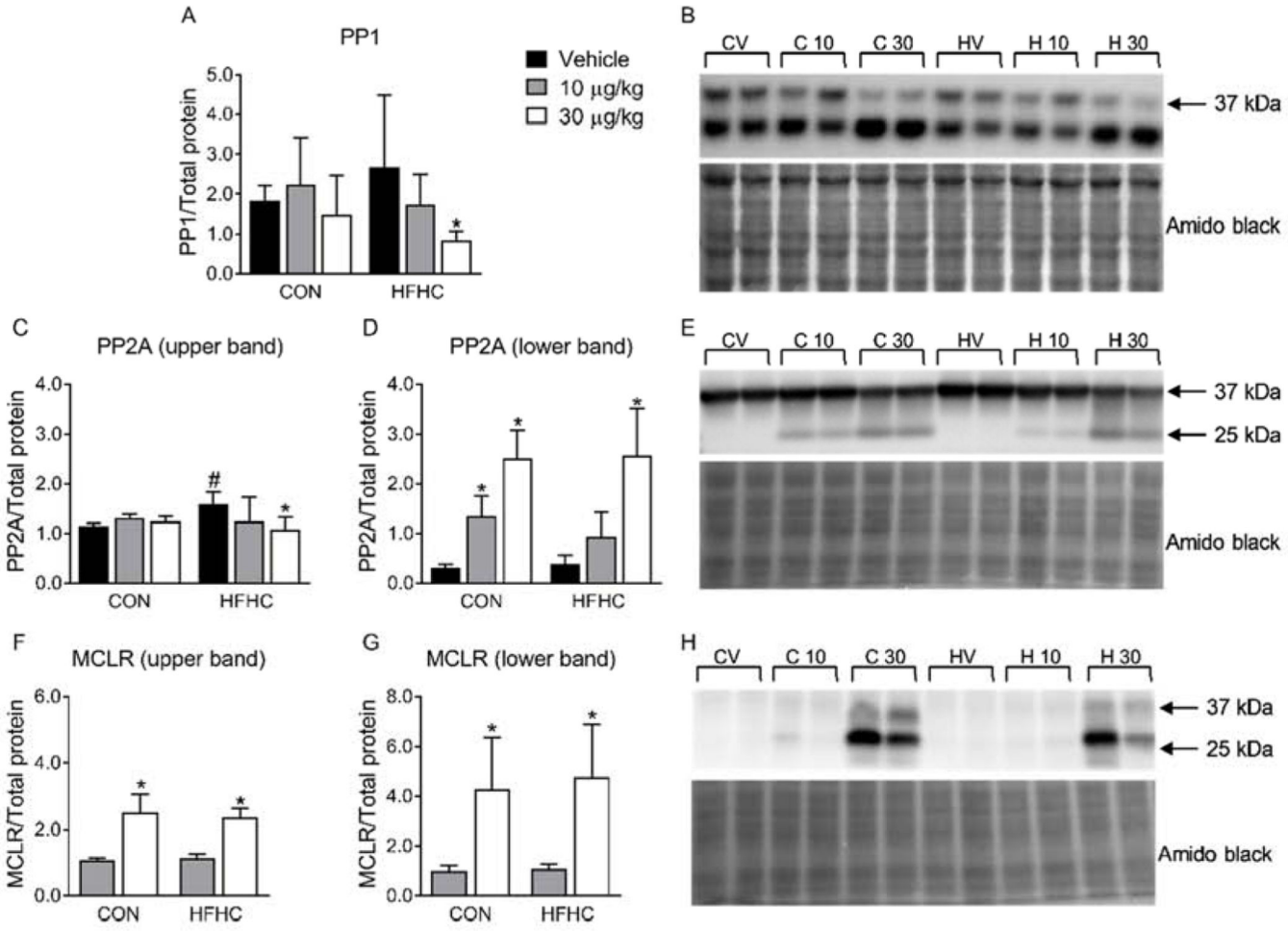

Figure 5:

Protein phosphatase and MCLR immunoblotting. (A) Densitometry of PP1 and (B) a representative western blot. (C) Densitometry of the upper PP2A and (D) lower PP2A bands along with (E) a representative western blot. (F) Densitometry of protein phosphatase bound upper and (G) lower MCLR bands along with (H) a representative western blot. Data represent mean ± SD. N = 6 for each group. Two-way ANOVA Dunnett multiple comparison post-test represented with (*) indicate p-value < 0.05 versus respective vehicle group. Two-way ANOVA Sidak multiple comparison post-test represented with (#) indicate p-value < 0.05 within each dose group.

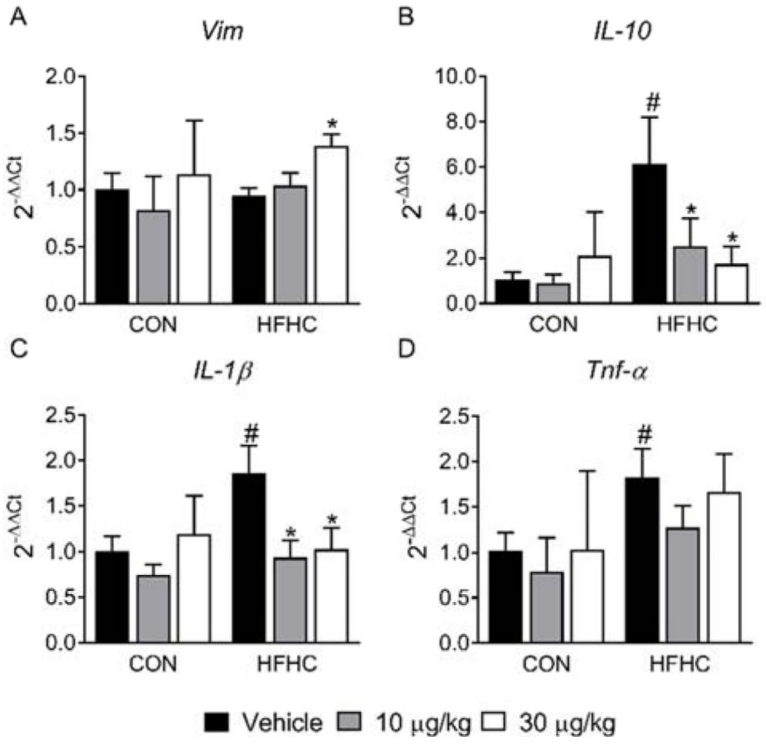

Figure 6:

Tubule regeneration and Inflammation. (A) *Vim* (Vimentin), (B) *IL-10*, (C) *IL-1β*, and (D) *Tnf-α* mRNA expression. Data represent mean ± SD. n = 6 per group. Two-way ANOVA Dunnett multiple comparison post-test represented with (*) indicate p-value < 0.05 versus respective vehicle group. Two-way ANOVA Sidak multiple comparison post-test represented with (#) indicate p-value < 0.05 within each dose group.

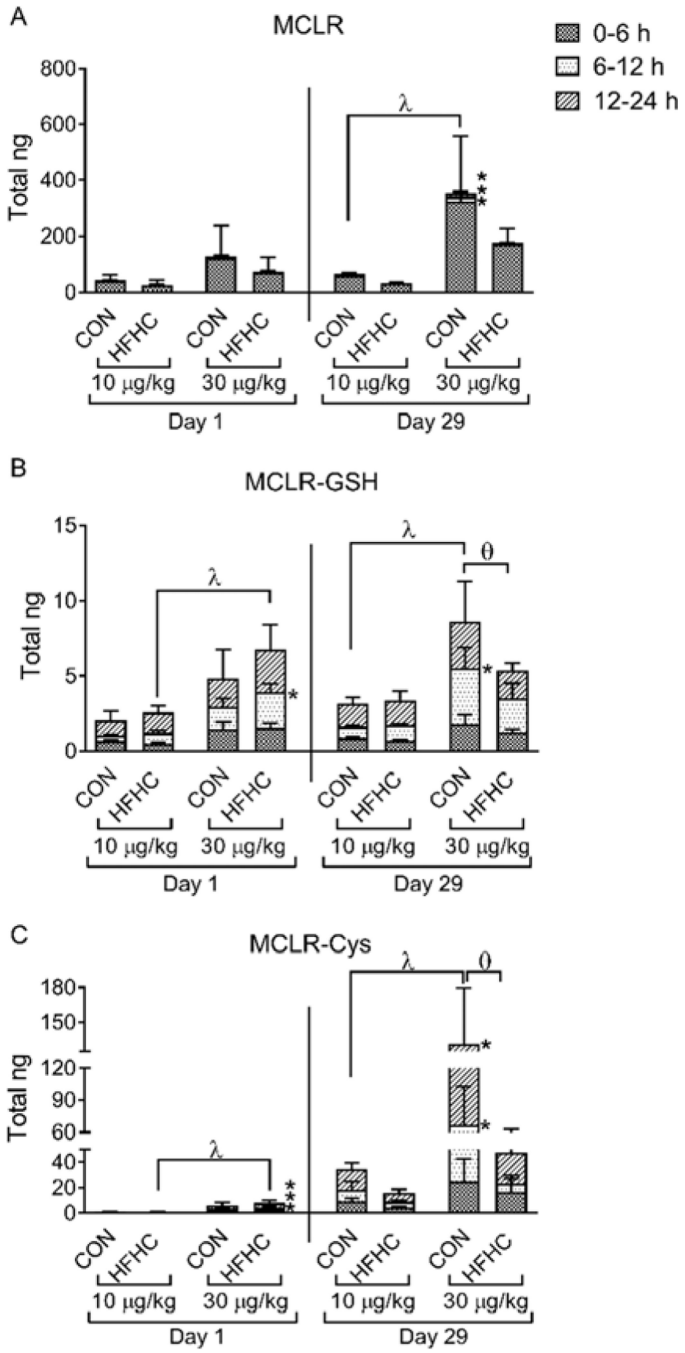

Figure 7:

MCLR metabolites. LC-MS/MS quantification of urinary elimination of (A) MCLR and MCLR metabolites (B) MCLR-GSH and (C) MCLR-Cys after a single dose (Day 1) and the final dose of MCLR (Day 29) divided into the urine collection time points (0–6, 6–12, 12–24 h). Data represent mean ± SD, n = 6 per group. Two-way ANOVA Dunnett multiple comparison post-test represented by * indicate p-value <0.05, *versus* respective vehicle group for each collection period (0–6, 6–12, or 12–24 h). Two-way ANOVA Dunnett multiple comparison post-test represented by (λ) indicate p-value < 0.05 *versus* respective

vehicle group for the complete 24-h period. Two-way ANOVA Sidak multiple comparison post-test represented with (ɵ) indicate p-value < 0.05 comparing control *versus* HFHC within each dose for the complete 24-h period.